Geochemistry Geophysics Geosystems G3

Article
Volume 13, Number 1
29 November 2012
Q0AF07, doi:10.1029/2012GC004211
ISSN: 1525-2027

Published by AGU and the Geochemical Society

Flux measurements of explosive degassing using a yearlong hydroacoustic record at an erupting submarine volcano

R. P. Dziak

Cooperative Institute for Marine Resources Studies, HMSC, Oregon State University/NOAA, 2115 SE OSU Drive, Newport, Oregon 97365, USA (robert.p.dziak@noaa.gov)

E. T. Baker

Pacific Marine Environmental Laboratory, National Oceanic and Atmospheric Administration, 7600 Sand Point Way NE, Seattle, Washington 98115, USA

A. M. Shaw

Geology and Geophysics Department, Woods Hole Oceanographic Institution, Woods Hole, Massachusetts 02543, USA

D. R. Bohnenstiehl

Department of Marine, Earth and Atmospheric Sciences, North Carolina State University, Campus Box 8208, Raleigh, North Carolina 27695, USA

W. W. Chadwick Jr., J. H. Haxel, and H. Matsumoto

Cooperative Institute for Marine Resources Studies, HMSC, Oregon State University/NOAA, 2115 SE OSU Drive, Newport, Oregon 97365, USA

S. L. Walker

Pacific Marine Environmental Laboratory, National Oceanic and Atmospheric Administration, 7600 Sand Point Way NE, Seattle, Washington 98115, USA

[1] The output of gas and tephra from volcanoes is an inherently disorganized process that makes reliable flux estimates challenging to obtain. Continuous monitoring of gas flux has been achieved in only a few instances at subaerial volcanoes, but never for submarine volcanoes. Here we use the first sustained (yearlong) hydroacoustic monitoring of an erupting submarine volcano (NW Rota-1, Mariana arc) to make calculations of explosive gas flux from a volcano into the ocean. Bursts of Strombolian explosive degassing at the volcano summit (520 m deep) occurred at 1–2 min intervals during the entire 12-month hydrophone record and commonly exhibited cyclic step-function changes between high and low intensity. Total gas flux calculated from the hydroacoustic record is 5.4 ± 0.6 Tg a^{-1}, where the magmatic gases driving eruptions at NW Rota-1 are primarily H_2O, SO_2, and CO_2. Instantaneous fluxes varied by a factor of ~100 over the deployment. Using melt inclusion information to estimate the concentration of CO_2 in the explosive gases as 6.9 ± 0.7 wt %, we calculate an annual CO_2 eruption flux of 0.4 ± 0.1 Tg a^{-1}. This result is within the range of measured CO_2 fluxes at continuously erupting subaerial volcanoes, and represents ~0.2–0.6% of the annual estimated output of CO_2 from all subaerial arc volcanoes, and ~0.4–0.6% of the mid-ocean ridge flux. The multiyear eruptive history of NW Rota-1 demonstrates that submarine volcanoes can be significant and sustained sources of CO_2 to the shallow ocean.

Components: 7900 words, 6 figures, 1 table.

Keywords: gas flux; ocean acoustics; seafloor volcanism.

Index Terms: 4259 Oceanography: General: Ocean acoustics; 8427 Volcanology: Subaqueous volcanism; 8428 Volcanology: Explosive volcanism (4302).

Received 25 April 2012; **Revised** 18 October 2012; **Accepted** 23 October 2012; **Published** 29 November 2012.

Dziak, R. P., E. T. Baker, A. M. Shaw, D. R. Bohnenstiehl, W. W. Chadwick Jr., J. H. Haxel, H. Matsumoto, and S. L. Walker (2012), Flux measurements of explosive degassing using a yearlong hydroacoustic record at an erupting submarine volcano, *Geochem. Geophys. Geosyst.*, *13*, Q0AF07, doi:10.1029/2012GC004211.

Theme: Assessing Magmatic, Neovolcanic, Hydrothermal, and Biological Processes along Intra-Oceanic Arcs and Back-Arcs

1. Introduction

[2] Most of Earth's volcanic activity occurs on the ocean floor, unobserved and undetected, at mid-ocean ridges where it is mostly effusive and at subduction zones where it is more likely explosive [e.g., *Rubin et al.*, 2012]. Records of explosive activity longer than a few weeks are rare even for subaerial volcanoes [*Garcés et al.*, 1998; *Hilton et al.*, 2002; *Johnson*, 2003; *Aiuppa et al.*, 2008] and nonexistent for submarine volcanoes. From February 2008 to February 2009, we recorded the first long-term, continuous hydroacoustic and volcanic plume record of an exploding submarine volcano, NW Rota-1. NW Rota-1 is a conical edifice rising ~2200 m from the surrounding seafloor [*Embley et al.*, 2006] within the recently established Marianas Trench Marine National Monument in the western Pacific Ocean (Figure 1a). A hydrophone and turbidity/temperature sensor, both moored ~150 m from the volcanic vent and 100 m off the seafloor (Figure 1b), provided an unprecedented yearlong view of the dynamic behavior of a Strombolian-style eruption on the deep seafloor.

[3] In this paper we use hydroacoustic explosion records at this submarine volcano to estimate the total explosive flux of gas from the summit vent. Our method is based on studies of infrasound arrivals at subaerial volcanoes [*Johnson*, 2003], but compensates for the different density, sound velocity, and sound pressure levels in the ocean. A correlation between acoustic signals and explosive degassing has been shown to exist at several subaerial, open-conduit volcanoes [*Firstov and Kravchenko*, 1996; *Vergniolle and Brandeis*, 1996; *Oshima and Maekawa*, 2001]. At Stromboli volcano, large (~1 m in diameter) gas bubbles exiting the magma column produced 10–30 Pa infrasound waves recorded at microphones a few hundred meters distant, and a near one to one correspondence between modeled and synthetic acoustic waveforms was achieved [*Vergniolle and Brandeis*, 1996]. The volatile bubbles at Stromboli are typically 80% H_2O, 10% CO_2, 5% H_2S and 5% Cl_2. Similarly, *Oshima and Maekawa* [2001] and *Firstov and Kravchenko* [1996] were able to generate highly accurate synthetic models of the infrasound (acoustic) records from the eruptive acceleration of compressed volatiles from the summit vents of Unzen and Klyuchevskoi, respectively.

[4] Two previous experiments have also attempted to correlate infrasound records of volcanic SO_2 gas flux with the flux observed using spectrometers coupled to telescopes and UV cameras [*McGonigle et al.*, 2009; *Dalton et al.*, 2010]. While *McGonigle et al.* [2009] observed good correlation between the SO_2 fluxes observed spectroscopically and irradiance captured by a thermal camera, these measurements were not well correlated with the infrasound data which was attributed to the strong directionality of the acoustic signals at Stromboli. *Dalton et al.* [2010] also used SO_2 emission data measured from a UV camera and coincident infrasound recordings over a two-hour period at Pacaya volcano (Guatemala) to calculate gas masses from both data sets. However, they found that the infrasound explosion fluxes had a high correlation (R^2 of 0.7) with the camera data during short duration (2–3 min) bubble-burst degassing events.

[5] Once an estimate of the explosive gas flux is made, flux estimates for a specific gas, such as CO_2, could be determined if its concentration in the exploded gas was known. However, quantitative

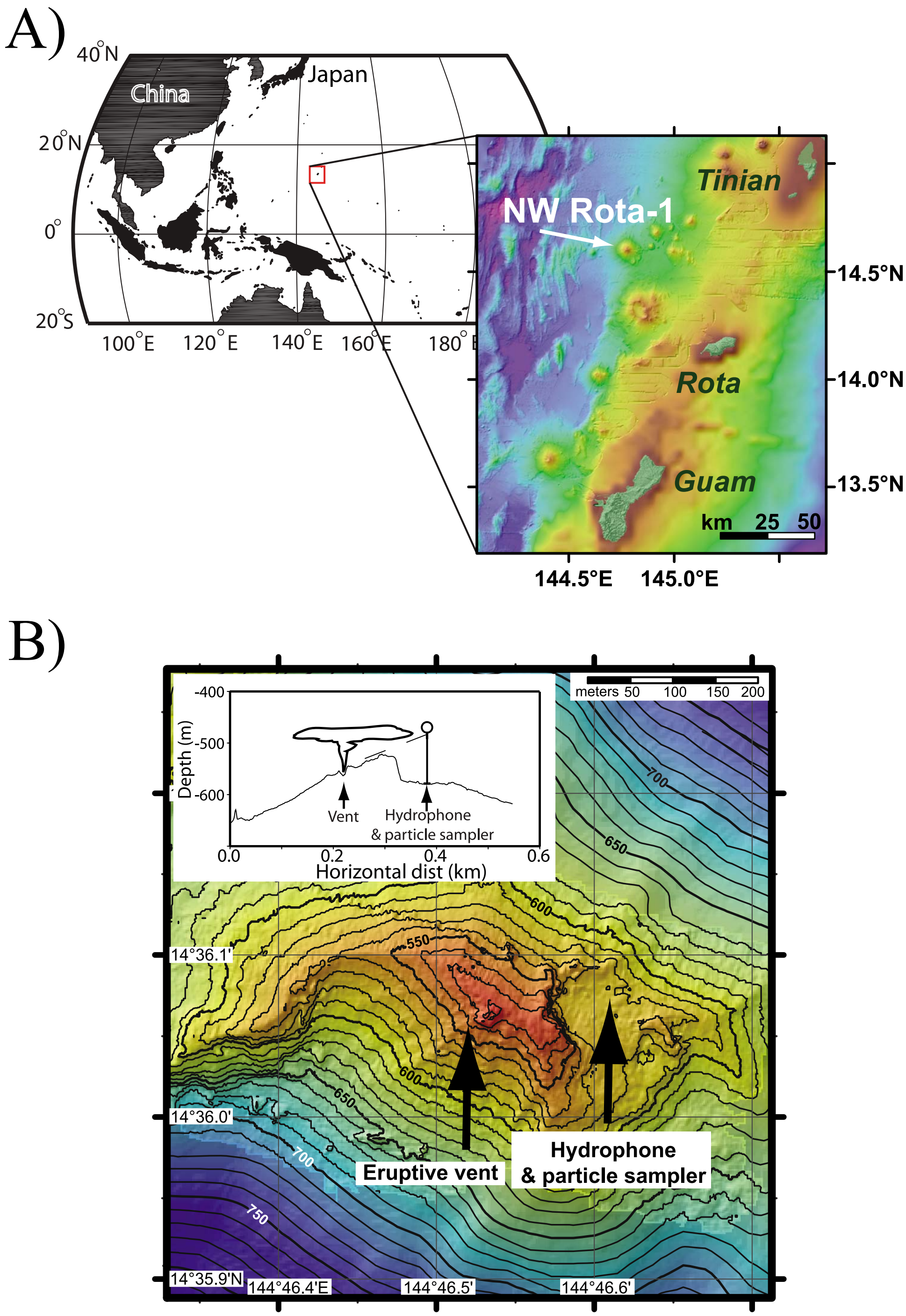

Figure 1. Bathymetric map and location of hydrophone mooring at NW Rota-1 volcano. (a) Regional map of NW Rota-1 in relation to Guam, Mariana Islands. (b) Bathymetry map of volcano summit showing location of eruption vent and hydrophone. Inset shows cross-section of relative depth between eruption vent and hydrophone mooring, with a clear acoustic line of sight between the two. The hydrophone is moored ~150 m from the volcanic vent and 100 m off the seafloor.

sampling of such gas is a daunting challenge at an erupting volcano. For this study we instead infer the CO_2 concentration from samples of melt inclusions from deep and seafloor summit rocks at NW Rota-1. Although this technique is admittedly first-order, even approximate CO_2 concentrations are a useful beginning for comparing the explosive CO_2 flux from a submarine volcano to the global database of degassing subaerial volcanoes.

2. NW Rota-1 Volcanic Explosions

[6] The eruption style observed at NW Rota-1 can be classified as submarine Strombolian, [*Chadwick et al.*, 2008a] where gas exists as a separate phase from the melt, effusive to explosive gas-driven eruption blasts last from 10 s of seconds to several minutes, and the produced volume of erupted tephra is relatively small (1–100 m^3/hr). The fundamental source of sound at Strombolian volcanoes is almost certainly the rapid release of pressurized gas at the free surface [*Vergniolle et al.*, 1996; *Rowe et al.*, 2000; *Johnson and Lees*, 2000]. This volcanic sound source arises from atmospheric pressure perturbations caused by the explosive outflow of volcanic volatiles, with gas fluxes on the order of 10^1 kg s^{-1} [*Newhall and Self*, 1982]. This eruption style has been confirmed at NW Rota-1 by both short-term video observations [*Chadwick et al.*, 2008a] and the long-term, continuous hydrophone recordings presented here. Moreover, in Strombolian eruptions the exsolving magmatic gas bubbles rise in the conduit, interacting and coalescing to form gas-rich and gas-poor zones. Between explosive bursts, seawater interacts with the top of the magma column to form a solid quench cap [*Chadwick et al.*, 2008a; *Deardorff et al.*, 2011]. Explosion bursts occur when the gas-rich zones reach the vent and the building gas pressure blows apart the solid quench cap. The violently expanding gas has sufficient velocity to entrain and transport molten and solid ejecta into the water column [*Deardorff et al.*, 2011]. Previous ROV dives at NW Rota have shown that the vast majority of degassing occurs at the eruptive vent, and is relatively minor at the diffuse hydrothermal vents elsewhere at the summit where the effluent is highly diluted [*Chadwick et al.*, 2008a; *Butterfield et al.*, 2011].

[7] During the 2008–2009 hydrophone deployment, the eruptive vent near the volcano's summit, at 520 m depth, exhibited near constant explosion signal packets (Figure 2a). These explosion packets lasted 60–120 s separated by quiescent intervals of 10–30 s over the entire 12 month record (Figure 2a). Each packet comprised hundreds of individual (100–200 ms duration) explosion pulses totaling ~12.7 million discrete pulses recorded during the year (Figure 2b, bottom). The acoustic explosion packets were broadband: 1–80 Hz with a peak at 30 Hz (Figure 3). The loudest explosions occurred during February to early June 2008 with a typical sound source level of 192 dB_{rms} re μPa^2/Hz @ 1 m, equal to ~100 W of acoustic power. This level is equivalent to the sound produced by an oceanic supertanker, and would be detectable at a range of ~100 km even during a Beaufort sea state of 6 [*Urick*, 1975]. The hydrophone record also documented a 1000-fold decrease in explosion intensity (amplitude) over the course of the year, marked by a sharp reduction after six months (in September 2008). This reduction in intensity of the acoustic explosion pulses likely reflects a decrease in explosivity at the vent, which may have been caused by a decrease in the rate of eruption and degassing, burial by accumulated ejecta, or other factors.

[8] Explosions at the summit vent also produced hundreds of individual plumes that carried ash and hydrothermal precipitates into the surrounding water column [*Resing et al.*, 2007; *Butterfield et al.*, 2011; *Deardorff et al.*, 2011], with no long periods of quiescence regardless of the explosion intensity (Figure 3). Most of the short-duration spikes recorded by the turbidity sensor, especially in the latter half of the record, were precursors to longer intervals of increased turbidity that lasted on the order of a day. The frequency of intense light-scattering pulses (Nephelometric Turbidity Units >4 [*American Public Health Association*, 1985]) increased sharply between August 15 and 30 2008, then lowered precisely when the explosion amplitude abruptly decreased at the beginning of September. This correlation is consistent with the hypothesis that an interval of higher eruptive output in late August changed the acoustic output of the eruptive vent by effectively burying it in debris. The connection between explosive intensity, acoustic amplitude, and plume production is apparent from ROV video recorded at the site in 2006 [*Chadwick, et al.*, 2008a], and our data are the first to confirm the frequent creation and dispersal of submarine volcanic plumes on a yearlong time scale.

3. Hydroacoustic Explosion Analysis

[9] We use the hydroacoustic explosion records to calculate the total explosive flux of gas from the summit vent (Figures 2b, 4, and 5). Our method is based on studies of infrasound arrivals at subaerial volcanoes [*Johnson*, 2003], but compensates for the different density, sound velocity, and sound pressure levels in the ocean. Cumulative gas flux is important because the total gas emission can be used as a proxy to characterize the cumulative magnitude of eruptive activity [*Johnson*, 2003; *Ripepe et al.*, 2007].

 10.1029/2012GC004211

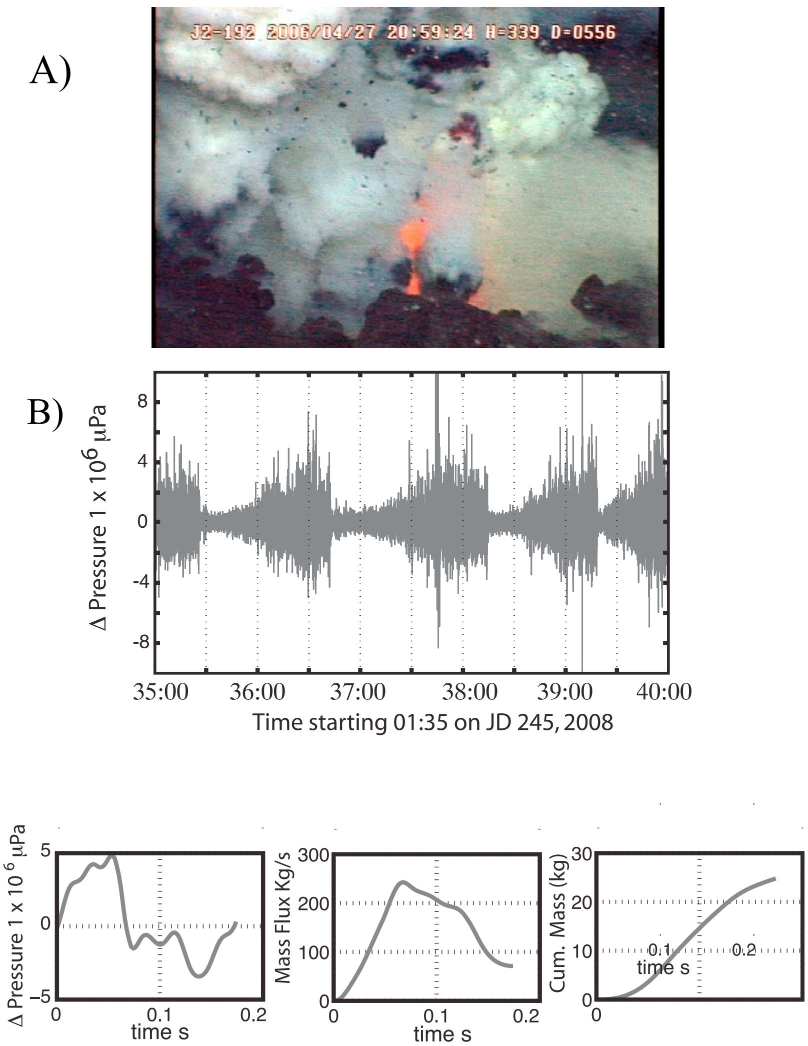

Figure 2. (a) Still image of magmatic explosion from summit vent in April 2006 [*Chadwick et al.*, 2008a]. (b) Top diagram shows September 2008 hydrophone record of five explosion signal packets, each packet is comprised of 100 s of individual explosion pulses. Bottom diagram shows (left to right) typical explosion pulse (~200 ms duration), mass flux of pulse calculated from equation (5), and cumulative mass (gas) flux of the pulse calculated using equation (6).

[10] Ocean sound consists of a regular motion of molecules in the water medium. Because water is a fluid, particle motion is communicated to adjacent particles and a sound wave is thereby propagated outward from a source at a speed equivalent to the sound velocity in water (c). The particle motion is parallel to the overall direction of propagation, and since ocean water is compressible, the particle motion causes changes in pressure that can be detected by a pressure sensitive hydrophone [*Urick*, 1975]. Thus the acoustic pressure recorded on the hydrophone is a time history of ocean pressure perturbations (ΔP) relative to background ocean pressure at the recording water depth. These excess ocean sound pressures are usually small (~10^{-3} Pa), and it has been the standard in the ocean acoustic literature to express sound pressure in decibels (dB) relative to a reference pressure (P_o) of 1 μPa [*Urick*, 1975]. Moreover, it is convention to use 1 m as the reference distance (r_o) when calculating the acoustic pressure of the source (written as dB re 1 μPa).

[11] The hydrophone used in this study records sound pressure changes in the deep ocean as proportional voltages. These signals are amplified, a 220 Hz low-pass anti-alias filter is applied, and the waveforms are digitized at a sample rate of 500 Hz before being stored on hard drives within the instrument pressure case.

[12] The recorded acoustic signal levels shown in Figures 2a and 4 were derived using the sonar equation [*Urick*, 1975]:

$$\mathrm{SL} = \mathrm{RL} + \mathrm{TL} - \mathrm{IR}, \quad (1)$$

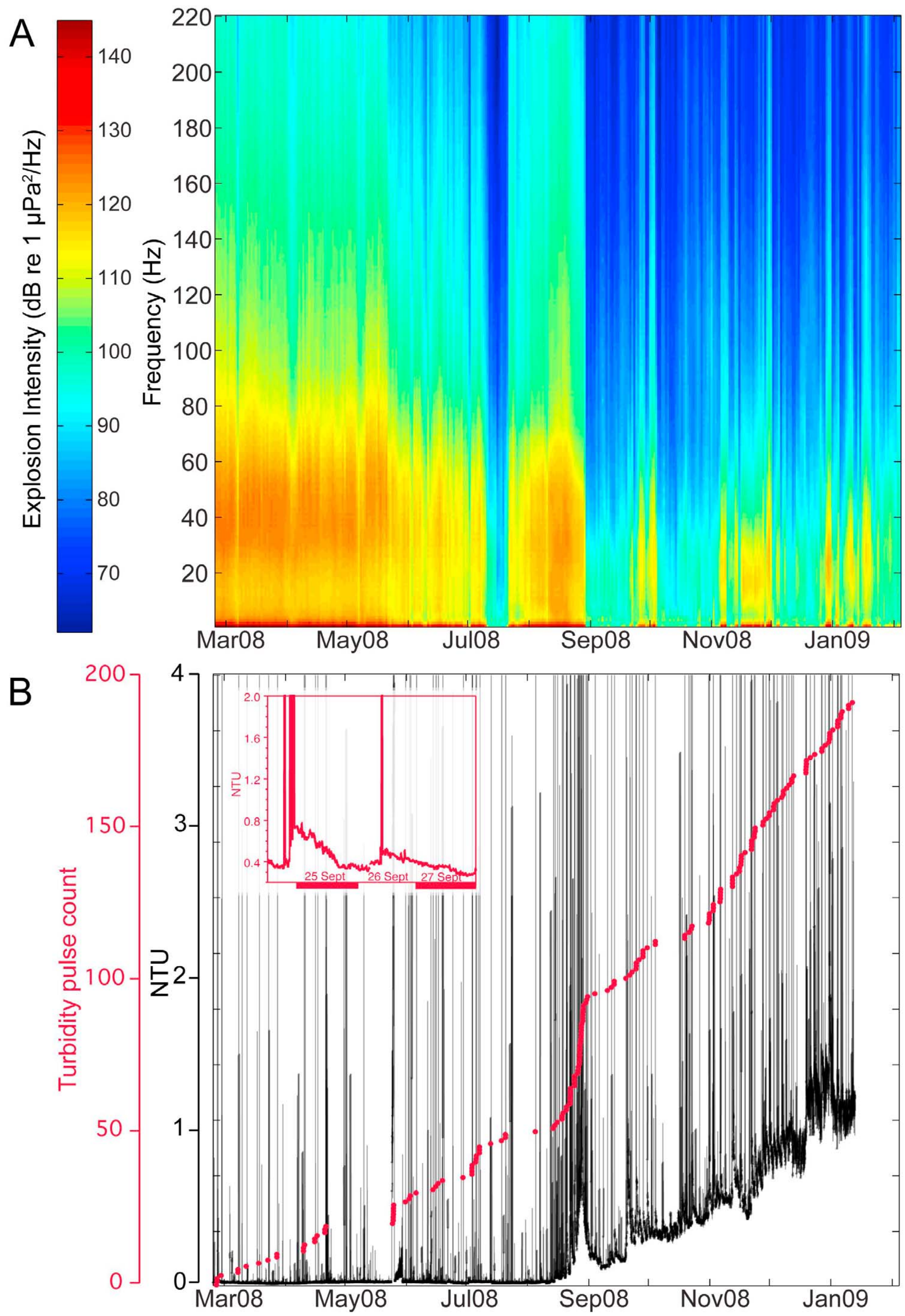

Figure 3. Hydrophone and eruption plume records from NW Rota-1 volcano. (a) Long-term, daily average, spectrogram of the hydrophone data (frequency in Hertz, amplitude intensity in decibels relative to 1 micro-Pascal^2/Hz) for the entire 12-month record. (b) Corresponding turbidity measurements in nephelometric turbidity units (NTU). NTU data (black line) were recorded every 15 min. The steady rise in baseline turbidity after September is interpreted to result from cumulative fouling of the optical lens. Red line shows time history of number of intense turbidity pulses (NTU > 4), perhaps of elemental S precipitates (e.g., as seen in *Embley et al.* [2006]). Inset shows how these pulses are normally followed by a longer-lasting period of increased turbidity. Because the turbidity pulses typically saturated the light-scattering sensor (5 V full scale), we cannot determine if the maximum turbidity correlates with explosion intensity. Even with quieter explosions, enough magmatic volatiles may be released to create a full-scale light-scattering response.

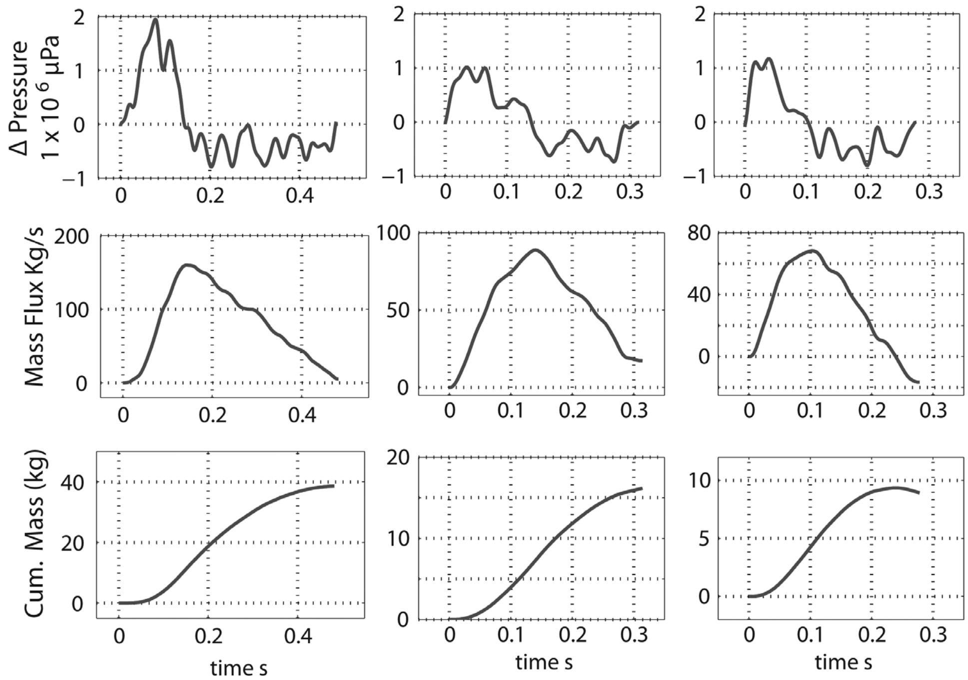

Figure 4. (top) Typical gas explosion pulses (200 ms duration) recorded on NW Rota-1 hydrophone. (middle) Mass flux calculated from each of the pulses using equation (5). (bottom) Cumulative gas flux of the pulses calculated using equation (6).

where RL is the acoustic received level recorded at the hydrophone, calculated as 10 $\log_{10}$ $(\Delta P/P_o)^2$ with units of dB re 1 μPa. IR is the frequency-dependent instrument response that accounts for the sensitivity of the hydrophone (-194 dB re 1V/μPa) and the gain of the amplifier. TL is the transmission loss (dB) over the acoustic propagation path. Since the hydrophone is very close to the sound source ($\sim$180 m slant range), we assume the acoustic signal is dominated by the volcanic explosion source, the signal undergoes only spherical spreading with negligible acoustic attenuation, and any distortion of the signal because of source directionality should be minimal. Unlike seismic propagation in the earth, ocean acoustic waveforms are relatively undistorted during propagation because the ocean does not support shear waves and is largely devoid of structures that scatter, attenuate, or reflect acoustic waves. Treating the source as a point source and applying the spherical spreading loss, the TL is then estimated as 20 $\log_{10}$ (r/r_0), where r is the distance from the source to the receiver and r_0 = 1 m. The source level SL therefore represents the acoustic pressure of the signal at a distance of 1 m from the source (dB re 1 μPa @ 1 m).

[13] Strombolian-style hydroacoustic signal generation at NW Rota-1 is relatively straightforward to model because: (1) a point source approximation is appropriate, because there is only one erupting vent, (2) vent diameter ($\sim$1 m [*Chadwick et al.*, 2008a]) is much less than the explosion sound wavelengths ($\sim$20–1500 m), (3) sound sources are primarily generated at the magma conduit/ocean interface and not within the magma column, (4) the elastic waves from the volcanic explosions are generated by the volatile gas bubble collapse as it

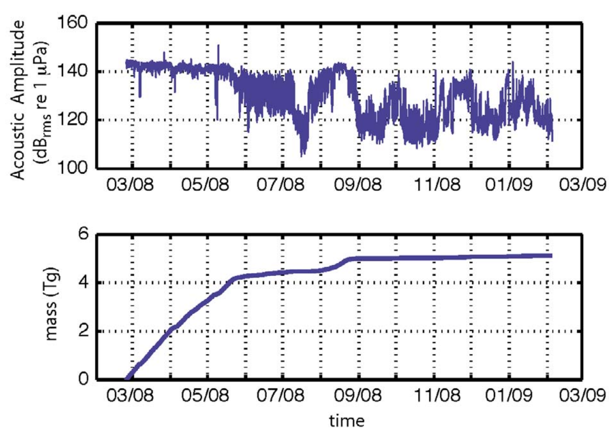

Figure 5. (top) Sound levels, root-mean square (rms) pressures in 1-h bins, recorded 150 m from the summit vent. (bottom) Cumulative gas flux calculated using equation (6), total as of February 2009 is 5.4 $\pm$ 0.6 Tga^{-1}. Note that the acoustic amplitude axis in the top panel is a log scale.

exits the magma at the vent-ocean interface, thus the bulk of the elastic wave energy is produced prior to the mixing of magmatic gases into seawater, and (5) ejection velocities are below the ocean sound speed and no shockwave is produced. The NW Rota-1 acoustic signals (Figures 2a, 2b, and 4) are clearly explosions and not jets; jet signals produce sustained band-limited tremor, whereas explosions result in broadband "N-wave" shaped waveforms [*Johnson and Lees*, 2000]. Thus the NW Rota-1 submarine volcanic sounds can be modeled as a simple or monopole source in a homogeneous medium, where the restoring force in the ocean is proportional to particle displacement. Acoustic compressional waves propagate elastically according to the wave equation [*Aki and Richards*, 2002]:

$$\nabla^2(\Delta P) - \frac{1}{c^2}\frac{\partial^2}{\partial t^2}(\Delta P) = -f(t)\,\partial(r), \qquad (2)$$

where $f(t)\,\partial(r)$ represents the source time force as a function of time t and the delta function $\partial(\mathrm{r})$ is zero everywhere except at $r = 0$. For spherical waves, a solution to the wave equation can then be written as [*Aki and Richards*, 2002]:

$$\Delta P = \frac{-f(t - r/c)}{4\pi\,\mathrm{r}}, \qquad (3)$$

For a simple acoustic point source in a homogeneous medium, the effective force function is equal to the rate of change of flux (mass outflow) from the source. Following the linear theory of sound, the excess pressure (ΔP) radiating into a half-space is given by [*Lighthill*, 1978]:

$$\Delta P = \frac{1}{2\pi r}\left(\frac{dq(t - r/c)}{dt}\right), \qquad (4)$$

where $q(t)$ is the mass flux from a point source at a distance r from the receiver, c is the speed of sound within the water column, and the $2\pi\mathrm{r}$ term accounts for geometric spreading of the pressure wave within a spherical half-space. The acoustic impedance of the fluid medium is inherently accounted for through conservation of momentum, and only the excess pressure, not the absolute pressure, enters into the calculation of mass flow.

4. Gas Flux Estimates

[14] Several approximations must be employed when estimating the flux of mass (or essentially gas in these volcanic explosion) values: (1) instrument response and ocean acoustic propagation effects are deconvolved, (2) the location of the hydroacoustic source is a point fixed at the vent, and (3) pressure perturbations at the source are small enough that a linear relationship exists between excess pressure, particle velocity, and particle displacement in the acoustic medium. Deconvolving the instrument response and acoustic propagation effects is standard practice in waveform analysis to estimate the physical parameters of the source. Moreover, the assumption of a point source is valid because the size of the vent is small ($\sim$1 m) as compared to the distance the acoustic waves propagate from the vent to the hydrophone ($\sim$150 m). Also since the excess ocean sound pressures in the NW Rota-1 explosions are relatively small ($\sim$1 Pa), there is very likely a linear relationship between excess pressure (ΔP) and particle velocity and displacement.

[15] From the recorded hydroacoustic pressure traces (Figures 2b, 4, and 5 (top)), the corresponding mass flux (kg s^{-1}) for a source of time duration (τ) may be approximated by:

$$q(t) = 2\pi r \int_0^{\tau} \Delta P(t + r/c)dt \qquad (5)$$

The cumulative flux $M(t)$ is then the time integral of the mass flux rate (Figure 5, bottom):

$$M(t) = \int_0^{\tau} 2\pi r \left[\int_0^{\tau} (\Delta P(t + r/c)dt\right] d\tau \qquad (6)$$

The hydroacoustic records should adequately represent cumulative explosive gas flux at NW Rota-1 because gas flow out of the summit vent was constantly turbulent (non-laminar), continually producing pressure waves. The cumulative flux mirrors the acoustic amplitudes (Figure 5), clearly showing a rapid gas release from March to early June 2008, another short increase during August, and a leveling off of gas flux rates beginning in September through the end of the record. In calculating cumulative gas flux we selected individual explosion pulses that exceed 1 Pa in amplitude and were between 150 and 2000 ms in duration, using both the positive and negative portions of the pulse amplitude (Figures 2b and 4). Using these criteria, a total of $\sim$12.7 million explosion pulses were detected from the NW Rota-1 hydrophone, and each discrete pulse was integrated using equation (5) and equation (6) to calculate the cumulative mass flux. As the hydrophone receiver is tethered above the seafloor, changes in the slant range between the receiver and vent, which are estimated to be on the order of $\pm$20 m, contribute the largest (11%) uncertainty to the mass calculation, making the total mass estimate 5.4 ± 0.6 Tg a^{-1}.

[16] The uncertainty in the calibration of the ITC 1032 hydrophone, as reported by the manufacturer, is ± 1 dB re 1 μPa, and there is perhaps another ± 1 dB re 1 μPa associated with the calibration of the instrument pre-amplifier. Hence the total uncertainty in the instantaneous pressure readings (σ_p) is on the order of 2 dB re 1 μPa (or 1.26×10^{-6} Pa). For the NW Rota data set this translates to a total uncertainty of ± 0.014 Tg of mass—a value that is negligible relative to the uncertainty in slant range.

[17] The hydroacoustic pulses integrated in this manner should adequately represent cumulative explosive gas flux at NW Rota-1, since the eruption is a series of gas explosions. The onsets of explosions at NW Rota-1 are highly impulsive, and because gas expansion accelerates dramatically at the onset, high-amplitude hydroacoustic excess pressures are generated. Thus these impulse signals may be used to determine a cumulative mass flux for the onset of an explosion. It is also important to note that the hydroacoustic record does not provide information on the rate that solid tephra debris is expelled into the water column since that process does not contribute to the acoustic signal recorded at the hydrophone.

[18] In most cases, accurate location of the explosion source is particularly important since volcanic systems can possess multiple active vents, e.g., Stromboli [*Ripepe et al.*, 2007]. However, seafloor observations before and after the hydrophone deployment confirm there is only one explosion vent at NW Rota-1 [*Chadwick et al.*, 2008a], and thus the only visible gas emissions are from this one explosive eruptive vent. It is also important to note that equation (6) refers to the cumulative mass flux of gas emitted from the volcanic vent and not to the mass of water displaced by the volumetric change of the source [*Lighthill*, 1978; *Johnson*, 2003]. Unfortunately, low-frequency contributions to the cumulative mass flux are often inadequately represented because laminar, steady state gas flow out of a vent should theoretically generate no sound [*Johnson*, 2003]. Because passive degassing is a common mechanism at most active volcanoes [*Sparks*, 1997], cumulative gas flux values recovered from infrasonic pressure records should be considered a lower limit or an estimate of a transient contribution.

5. Estimating CO_2 Flux

[19] We next turn to the more challenging problem of estimating the concentration of CO_2 in the explosive gas. It is known that the magmatic gases driving the eruptions at NW Rota-1 are primarily H_2O, SO_2, and CO_2 [*Resing et al.*, 2007; *Chadwick et al.*, 2008a; *Lupton et al.*, 2008; *Butterfield et al.*, 2011], but we had no sampling capability to directly measure their exact proportions and quantities at the vent. Instead, we estimate the composition of gas emitted at NW Rota-1 by comparing volatile concentrations measured in melt inclusions trapped within olivine crystals at deep depths ($\sim$5.2 km) to those trapped at shallow depths at or near the eruption site. H_2O, CO_2, and SO_2 species are the main volatile phases that degas from the melt as it ascends, and their concentrations in the melt inclusions range from 1.4 to 2.8 wt%, 5–460 ppm, and 535–800 ppm, respectively [*Shaw et al.*, 2006], where the associated errors are on the order of 10% [*Shaw et al.*, 2010]. Thus by subtracting the lowest melt compositions (trapped at the seafloor) from the highest values (from a relatively deep undegassed source), we calculate that the expelled gas contains 3.1 mol % or 6.9 ± 0.7 wt % CO_2, within the range ($\sim$1–10%) found at other volcanoes along subduction zones [*Symonds et al.*, 1994]. The similarity between previous measurements of the S/C mole ratio in the NW Rota-1 plume, 1.4 [*Resing et al.*, 2007], and the S/C mole ratio derived from the melt inclusions, 0.8, supports our melt inclusion approach. S/C ratios can vary during an eruption cycle, but rarely more than an order of magnitude [e.g., *Hobbs et al.*, 1991; *Doukas*, 1995; *Aiuppa et al.*, 2008]. The average S/C ratio from high-temperature fumaroles across 11 volcanic arcs is 0.8 ± 1.3 [*Fischer*, 2008], the same as our value from melt inclusions. This close agreement is somewhat fortuitous but does imply that our S/C value is reasonable.

[20] As previously noted, the hydroacoustic record does not provide information on the rate that solid debris is expelled into the water column, most of which is ultimately moved down the steep south flank of the volcano by gravity flows [*Walker et al.*, 2008; *Deardorff et al.*, 2011; *Chadwick et al.*, 2012]. Also, because the mass flux is a measure of gas emitted from the volcanic vent and not the mass of water displaced by the volumetric change, in our view it is not necessary to correct our mass flux estimate for the gas density of the three major volatiles comprising the total gas volume.

[21] We thus use the total flux of explosively released gas from NW Rota-1, 5.4 ± 0.6 Tg a^{-1}, to calculate an explosive CO_2 flux of 0.4 ± 0.1 Tg a^{-1}, using the errors associated with the calculations of total gas flux and the CO_2 fraction of the gas. This estimate is a minimum, as some CO_2

degassing could have occurred prior to melt inclusion entrapment (i.e., the original source could have had even higher CO_2). A highly conservative approach to the error assessment is to calculate the range of CO_2 flux using the observed range of ~1–10% CO_2 in volcanic gases from other arc volcanoes [*Symonds et al.*, 1994]. This calculation yields a CO_2 flux range of 0.05–0.54 Tg a^{-1}.

[22] Our estimate does not include CO_2 vented by non-eruptive hydrothermal discharge. At NW Rota-1, water column measurements indicate two CO_2 plumes originating from the summit region: a high-rising plume rich in CO_2 associated with explosive eruptions, and a deeper plume with lower CO_2 apparently derived from passive fluid discharge from low-temperature vent fields [*Resing et al.*, 2007]. There is no evidence for gas venting on the volcano's flanks [*Walker et al.*, 2008]. No hydrothermal tracers (e.g., ^{3}He, dissolved Mn and Fe) have been detected in waters around the flanks, and measured ΔCO_2 below the summit is $\sim\pm1$ μM (measured plume values range up to 50 μM [*Resing et al.*, 2007]). The balance between eruptive and passive flux has not been quantified at NW Rota-1, but vertical profiles through both plumes find substantially higher CO_2 concentrations in the eruption plume. This assumption is consistent with measurements at subaerial volcanoes, where diffuse degassing typically contributes $<\sim10\%$ of the CO_2 flux at erupting (i.e., open conduit) arc volcanoes [e.g., *D'Alessandro et al.*, 1997; *Carapezza and Federico*, 2000; *Wardell et al.*, 2001; *Varley and Armienta*, 2001]. Thus we consider explosive eruptions to be the major source of CO_2 from NW Rota-1.

6. Discussion

[23] Our estimated explosive CO_2 flux from NW Rota-1 falls within the broad range, <0.01 to >30 Tg a^{-1}, established from measurements at individual arc or near-arc subaerial volcanoes (Table 1). This compilation shows that eruptive basaltic/andesitic volcanoes, such as NW Rota-1, are distinguished by CO_2 fluxes that are consistently higher ($>\sim0.5$ Tg a^{-1}) and more variable than quiescent volcanoes. During an eruption cycle, CO_2 fluxes can easily vary by one or more orders of magnitude (e.g., Etna, Redoubt, Augustine, NW Rota-1 (Table 1)), so occasional discrete measurements can provide misleading information about CO_2 output on a long-term basis. At Etna, for example, a rare continuous time series of CO_2 emissions during a several month eruption cycle found fluxes repeatedly fluctuating between ~0.4 and >24 Tg a^{-1} (Figure 6a), a cycling only crudely approximated by concurrent discrete sampling [*Aiuppa et al.*, 2008]. Highly variable gas flux has also been documented at erupting volcanoes such as St. Augustine [*Symonds et al.*, 1992], Spurr [*Doukas*, 1995], Stromboli [*Allard et al.*, 1994], Galeras [*Zapata G et al.*, 1997] and others. Our observations at NW Rota-1 (Figure 6b) display a similar scale of variability. Published exceptions to such variability occur only when the number of observations is small and the volcano is not in an eruptive phase (e.g., White Island and other quiescent volcanoes). The absence of variability estimates from studies at many volcanoes (Table 1) underscores the difficulty of obtaining representative long-term measurements. Uncertainties about the CO_2 flux from volcanoes thus arise directly from the challenge of conducting continuous, long-term, and integrative gas flux measurements.

[24] Hydroacoustic monitoring of submarine volcanoes makes such measurements practical. Our best estimate of the mean explosive CO_2 flux at NW Rota-1, 0.4 ± 0.1 Tg a^{-1}, was at the low end of subaerial eruptive volcanoes but substantially greater than almost all measurements at quiescent volcanoes. Its low flux relative to erupting subaerial volcanoes is not surprising given that most subaerial measurements target volcanoes with large calderas and correspondingly large magmatic heat sources. Although the instantaneous explosive CO_2 flux at NW Rota-1 varied by a factor of ~100 over the deployment, our continuous monitoring provided a robust estimate of the cumulative flux with a relatively small error estimate (25%).

[25] On the global scale, estimates of the total eruptive output of CO_2 from subaerial arc volcanoes range from ~70–250 Tg a^{-1} [*Hilton et al.*, 2002; *Williams et al.*, 1992; *Mörner and Etiope*, 2002; *Fischer*, 2008]. The total volcanic supply of CO_2 to the ocean is also uncertain. The flux from the entire mid-ocean ridge system has been estimated at ~70–100 Tg a^{-1} [*Shaw et al., 2010*; *Sano and Williams*, 1996; *Marty and Tolstikhin*, 1998], but there is no comparable estimate from submarine arc volcanoes. Our best estimate of CO_2 from NW Rota-1, 0.4 ± 0.1 Tg a^{-1}, represents ~0.2–0.6% of the annual estimated output of CO_2 from all subaerial arc volcanoes, and ~0.4–0.6% of the mid-ocean ridge flux. The only previous estimate of CO_2 flux at a submarine arc volcano comes from non-erupting NW Eifuku (in the northern Mariana arc), where liquid CO_2 was observed leaking as buoyant droplets at a rate of 0.035 Tg a^{-1} [*Lupton et al.*, 2006]. This flux is comparable to that from the quiescent volcanoes in Table 1 (median =

Table 1. CO_2 Flux Measurements at Erupting and Quiescent Arc Volcanoes

	CO_2 $(\pm 1\sigma)^a$ (Tg a^{-1})	Most Recent Eruption[d]	Measurement Type	References
		Erupting Volcanoes		
Etna	3.6–32.8	2011	Eruptive plumes	*Aiuppa et al.* [2008]
Etna	2 ± 1.8	2011	Non-eruptive plumes	*Aiuppa et al.* [2008]
Redoubt	15 ± 19	2009	Eruptive plumes	*Casadevall et al.* [1994]; *Hobbs et al.* [1991]
Redoubt	0.60 ± 0.3	2009	Post-eruptive plumes	*Casadevall et al.* [1994]; *Hobbs et al.* [1991]
Augustine	2.5 ± 0.4	2006	Eruptive plumes	*Symonds et al.* [1992]
Augustine	0.003 ± 0.06	2006	Non-eruptive plumes	*Symonds et al.* [1992]
Popocatepetl	2.2	2011	Non-eruptive plumes (magmatic CO_2 only)	*Goff et al.* [2001]
Cerro Negro	2.0	1999	Diffuse degassing	*Salazar et al.* [2000]
St Helens	0.4–4	2008	Eruptive and non-eruptive plumes	*Casadevall et al.* [1983]
Stromboli	1.1–2.1 (0.6–1.2)[b]	2011	Eruptive and non-eruptive plumes	*Allard et al.* [1994]
Masaya	1–1.1	2008	Non-eruptive plumes	*Burton et al.* [2000]
Spurr	1 ± 1.3	1992	Eruptive and non-eruptive plumes	*Doukas* [1995]
White Is	0.95 ± 0.02	2001	Non-eruptive plumes	*Wardell et al.* [2001]
Rabaul	0.9	2011	Diffuse degassing	*Pérez et al.* [1998]
Galeras	0.37 ± 0.33	2010	Eruptive and non-eruptive plumes	*Zapata G et al.* [1997]
NW Rota-1	0.4 ± 0.1	Ongoing	Eruptive plumes	This paper
		Quiescent Volcanoes		
Solfatara di Pozzouli	0.555 (0.4–0.8, 90%CI)[c]	1538	Diffuse gassing	*Cardellini et al.* [2003]
Ischia	0.479	1302	Diffuse gassing	*Pecoraino et al.* [2005]
Ustica	0.26 ± 0.18	Pleistocene	Diffuse gassing	*Etiope et al.* [1999]
Vulcano	0.18	1890	Diffuse gassing, fumaroles	*Inguaggiato et al.* [2012]
Albani Hills	0.19	>10 K BCE	Diffuse gassing	*Chiodini and Frondini* [2001]
Vulcano	0.095	1890	Diffuse gassing	*Chiodini et al.* [1996]
Usu	0.06 ± 0.06	2001	Diffuse gassing	*Hernández et al.* [2001a]
Miyakejima	0.045 ± 0.012	2010	Diffuse gassing	*Hernández et al.* [2001b]
Nisyros	0.031	1888	Diffuse gassing, fumaroles	*Cardellini et al.* [2003]
Hakkoda	0.027	1550	Diffuse gassing	*Hernández Perez et al.* [2003]
Iwoyama	0.003	1768	Diffuse gassing, fumaroles	*Mori et al.* [2001]

[a]±1 standard deviation about the mean, when available from the source.
[b]Means and ranges only given.
[c]90% confidence interval.
[d]*Siebert and Simkin* [2002].

0.095 Tg a^{-1}). The CO_2 output from NW Eifuku has a measurable ecological impact as it has been shown to hinder shell development of local chemosynthetic mussels [*Tunnicliffe et al.*, 2009]. The almost continuous eruption of NW Rota-1 since at least 2003 [*Embley et al.*, 2006; *Chadwick et al.*, 2012] injects an even larger and sustained source of CO_2 into the shallow ocean that could have similarly significant biological impacts. Two other submarine volcanoes in the Mariana arc (Nikko and Daikoku) and two in the Tonga-Kermadec arc (Giggenbach and Volcano-1) have recently been shown to also be discharging CO_2 -rich bubbles [*Lupton et al.*, 2008]. Although CO_2 flux has not yet been estimated from these volcanoes, their presence indicates that carbon fluxes from submarine arcs may be significant. Thus although the explosive CO_2 flux from NW Rota-1 is only a small fraction of the flux from subaerial arc volcanoes, the total CO_2 flux from all submarine volcanoes may be a substantial fraction of the flux from subaerial volcanoes and mid-ocean ridges.

[26] Remote hydroacoustic measurements make the monitoring of many volcanoes a quantitative and economically feasible approach to the study of volatile output from submarine arcs. Two other submarine volcanoes with long-lived eruptive activity are already known. Hydroacoustic *T* waves have been detected at Monowai, at 25°45′S on the Kermadec arc, for more than 30 years [*Kibblewhite*, 1966; *Talandier and Okal*, 1987; *Wright et al.*, 2008; *Chadwick et al.*, 2008b; *Watts et al.*, 2012]. Lava eruptions and magmatic gas explosions were observed at West Mata, at 15°5.7′S on the Tonga arc in 2009 [*Resing et al.*, 2011]. More erupting

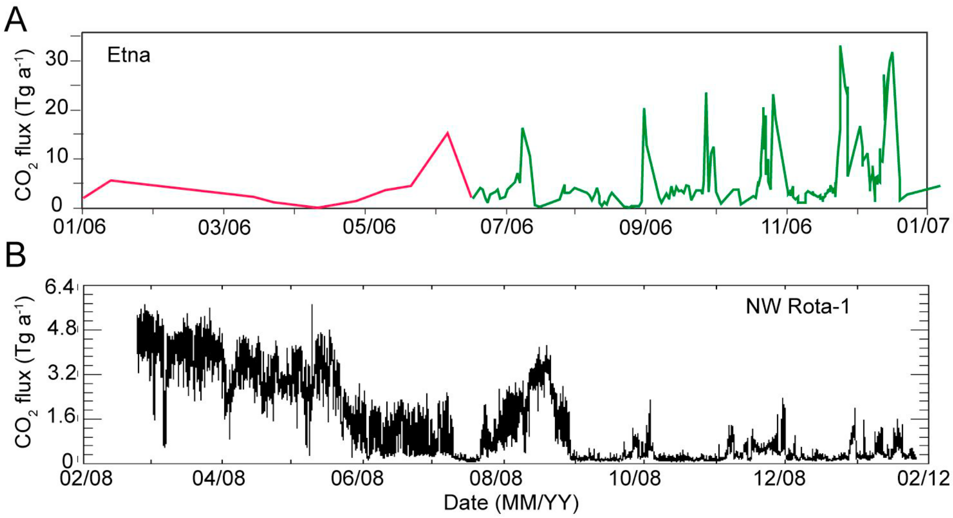

Figure 6. Comparison of time series measurements of CO_2 flux from Mt. Etna and acoustically estimated flux from NW Rota-1. (a) At Etna, discrete, bimonthly measurements (red line) were performed for the first half of 2006, followed by continuous (green line, four 30-min-duration measurements/day) later in 2006 when explosive activity became common [*Aiuppa et al.*, 2008]. (b) At NW Rota-1 the CO_2 flux was estimated from data recorded every second.

submarine volcanoes certainly lie undiscovered on other, less explored, arcs. Our results from NW Rota-1 demonstrate that quantifying the global contribution of CO_2 from submarine volcanic arcs depends not only on the enumeration of all hydrothermal sources, but also on the discovery of sites of volcanically controlled gas discharge.

Acknowledgments

[27] We thank the USCG M/V *Sequoia*, the National Oceanic and Atmospheric Administration Office of Ocean Exploration and Research, the NOAA Vents Program, and the National Science Foundation (OCE-0751776) for support. We also thank M. Fowler for mooring recoveries, T.-K. Lau for programming and S. Merle for graphics support. The authors wish to thank P. Michael, K. Rubin, M. Tolstoy, and T. Thordarson for very helpful comments that improved the manuscript. PMEL contribution 3435.

References

Aiuppa, A., et al. (2008), Total volatile flux from Mount Etna, *Geophys. Res. Lett.*, *35*, L24302, doi:10.1029/2008GL035871.

Aki, K., and P. Richards (2002), *Quantitative Seismology*, Univ. Sci. Books, Sausalito, Calif.

Allard, P., J. Carbonnelle, N. Métrich, H. Loyer, and P. Zettwoog (1994), Sulphur output and magma degassing budget of Stromboli volcano, *Nature*, *368*, 326–330, doi:10.1038/368326a0.

American Public Health Association (1985), *Standard Methods for the Examination of Water and Wastewater*, 16th ed., Washington, D. C.

Burton, M. R., C. Oppenheimer, L. A. Horrocks, and P. W. Francis (2000), Remote sensing of CO_2 and H_2O emission rates from Masaya volcano, Nicaragua, *Geology*, *28*(10), 915–918, doi:10.1130/0091-7613(2000)28<915:RSOCAH>2.0.CO;2.

Butterfield, D. A., K. Nakamura, B. Takano, M. D. Lilley, J. E. Lupton, J. A. Resing, and K. K. Roe (2011), High SO_2 flux, sulfur accumulation and gas fractionation at an erupting submarine volcano, *Geology*, *39*(9), 803–806, doi:10.1130/G31901.1.

Carapezza, M. L., and C. Federico (2000), The contribution of fluid geochemistry to the volcano monitoring of Stromboli, *J. Volcanol. Geotherm. Res.*, *95*, 227–245, doi:10.1016/S0377-0273(99)00128-6.

Cardellini, C., G. Chiodini, and F. Frondini (2003), Application of stochastic simulation to CO_2 flux from soil: Mapping and quantification of gas release, *J. Geophys. Res.*, *108*(B9), 2425, doi:10.1029/2002JB002165.

Casadevall, T., W. Rose, T. Gerlach, L. P. Greenland, J. Ewert, R. Wunderman, and R. Symonds (1983), Gas Emissions and the eruptions of Mount St. Helens through 1982, *Science*, *221*, 1383–1385, doi:10.1126/science.221.4618.1383.

Casadevall, T. J., M. P. Doukas, C. A. Neal, R. G. McGimsey, and C. A. Gardner (1994), Emission rates of sulfur dioxide and carbon dioxide from Redoubt Volcano, Alaska during the 1989–1990 eruptions, *J. Volcanol. Geotherm. Res.*, *62*, 519–530, doi:10.1016/0377-0273(94)90050-7.

Chadwick, W. W., Jr., K. V. Cashman, R. W. Embley, H. Matsumoto, R. P. Dziak, C. E. J. de Ronde, T.-K. Lau, N. Deardorff, and S. G. Merle (2008a), Direct video and hydrophone observations of submarine explosive eruptions, *J. Geophys. Res.*, *113*, B08S10, doi:10.1029/2007JB005215.

Chadwick, W. W., Jr., I. C. Wright, U. Schwarz-Schampera, O. Hyvernaud, D. Reymond, and C. E. J. De Ronde (2008b), Cyclic eruptions and sector collapses at Monowai submarine volcano, Kermadec arc: 1998–2007, *Geochem. Geophys. Geosyst.*, *9*, Q10014, doi:10.1029/2008GC002113.

Chadwick, W. W., Jr., R. P. Dziak, J. H. Haxel, R. W. Embley, and H. Matsumoto (2012), Submarine landslide triggered by volcanic eruption recorded by in-situ hydrophone, *Geology*, *40*(1), 51–54, doi:10.1130/G32495.1.

Chiodini, G., and F. Frondini (2001), Carbon dioxide degassing from the Albani Hills volcanic region, Central Italy, *Chem. Geol.*, *177*, 67–83, doi:10.1016/S0009-2541(00)00382-X.

Chiodini, G., F. Frondini, and B. Raco (1996), Diffuse emission of CO_2 from the Fossa crater, Vulcano Island (Italy), *Bull. Volcanol.*, *58*, 41–50, doi:10.1007/s004450050124.

D'Alessandro, W., S. Giammanco, F. Parello, and M. Valenza (1997), CO_2 output and $\delta^{13}C(CO_2)$ from Mount Etna as indicators of degassing of shallow asthenosphere, *Bull. Volcanol.*, *58*, 455–458, doi:10.1007/s004450050154.

Dalton, M. P., G. P. Waite, I. M. Watson, and P. A. Nadeau (2010), Multiparameter quantification of gas release during weak Strombolian eruptions at Pacaya Volcano, Guatemala, *Geophys. Res. Lett.*, *37*, L09303, doi:10.1029/2010GL042617.

Deardorff, N. D., K. V. Cashman, and W. W. Chadwick Jr. (2011), Observations of eruptive plumes and pyroclastic deposits from submarine explosive eruptions at NW Rota-1, Mariana Arc, *J. Volcanol. Geotherm. Res.*, *202*(1–2), 47–59, doi:10.1016/j.jvolgeores.2011.01.003.

Doukas, M. P. (1995), A compilation of sulfur dioxide and carbon dioxide emission-rate data from Cook Inlet volcanoes (Redoubt, Spurr, Iliama and Augustine), Alaska, during the period from 1990 to 1994, *U.S. Geol. Surv. Open File Rep.*, *95-55*, 18 pp.

Embley, R. W., et al. (2006), Long-term eruptive activity at a submarine arc volcano, *Nature*, *441*, 494–497, doi:10.1038/nature04762.

Etiope, G., P. Beneduce, M. Calcara, P. Favali, F. Frugoni, and M. Schiattarella (1999), Structural pattern and CO_2-CH_4 degassing of Ustica Island, S. Tyrrhenian basin, *J. Volcanol. Geotherm. Res.*, *88*, 291–304.

Firstov, P. P., and N. M. Kravchenko (1996), Estimation of the amount of explosive gas released in volcanic eruptions using air waves, *Volcanol Seismol.*, *17*, 547–560.

Fischer, T. P. (2008), Fluxes of volatiles (H_2O, CO_2, N_2, Cl F) from arc volcanoes, *Geochem. J.*, *42*, 21–38, doi:10.2343/geochemj.42.21.

Garcés, M., M. T. Hagerty, and S. Y. Schwartz (1998), Magma acoustics and time-varying melt properties at Arenal Volcano, Costa Rica, *Geophys. Res. Lett.*, *25*(13), 2293–2296, doi:10.1029/98GL01511.

Goff, F., S. P. Love, R. G. Warren, D. Counce, J. Obenholzner, C. Siebe, and S. C. Schmidt (2001), Passive infrared remote sensing evidence for large, intermittent CO_2 emissions at Popocatepetl volcano, Mexico, *Chem. Geol.*, *177*, 133–156, doi:10.1016/S0009-2541(00)00387-9.

Hernández, P. A., K. Notsu, J. M. Salazar, T. Mori, G. Natale, H. Okada, G. Virgili, Y. Shimoike, M. Sato, and N. M. Pérez (2001a), Carbon dioxide degassing by advective flow from Usu volcano, Japan, *Science*, *292*, 83–86, doi:10.1126/science.1058450.

Hernández, P. A., J. M. Salazar, Y. Shimoike, T. Mori, K. Notsu, and N. Pérez (2001b), Diffuse emission of CO_2 from Miyakejima volcano, Japan, *Chem. Geol.*, *177*, 175–185, doi:10.1016/S0009-2541(00)00390-9.

Hernández Perez, P., K. Notsu, M. Tsurumi, T. Mori, M. Ohno, Y. Shimoike, J. Salazar, and N. Pérez (2003), Carbon dioxide emissions from soils at Hakkoda, north Japan, *J. Geophys. Res.*, *108*(B4), 2210, doi:10.1029/2002JB001847.

Hilton, D. R., et al. (2002), Noble gases and volatile recycling at subduction zones, *Rev. Mineral. Geochem.*, *47*, 319–370, doi:10.2138/rmg.2002.47.9.

Hobbs, P. V., L. F. Radke, J. H. Lyons, R. J. Ferek, D. J. Coffman, and T. J. Casadevall (1991), Airborne measurements of particle and gas emissions from the 1990 volcanic eruptions of Mount Redoubt, *J. Geophys. Res.*, *96*, 18,735–18,752, doi:10.1029/91JD01635.

Inguaggiato, S., A. Mazot, I. S. Diliberto, C. Inguaggiato, P. Madonia, D. Rouwet, and F. Vita (2012), Total CO_2 output from Vulcano island (Aeolian Islands, Italy), *Geochem. Geophys. Geosyst.*, *13*, Q02012, doi:10.1029/2011GC003920.

Johnson, J. B. (2003), Generation and propagation of infrasonic airwaves from volcanic explosions, *J. Volcanol. Geotherm. Res.*, *121*, 15–63, doi:10.1016/S0377-0273(02)00409-2.

Johnson, J. B., and J. M. Lees (2000), Plugs and chugs—Seismic and acoustic observations of degassing explosions at Karymsky, Russia and Sangay, Ecuador, *J. Volcanol. Geotherm. Res.*, *101*, 67–82, doi:10.1016/S0377-0273(00)00164-5.

Kibblewhite, A. C. (1966), Detection and location of a new underwater volcano, *Nature*, *210*, 938–939, doi:10.1038/210938a0.

Lighthill, M. J. (1978), *Waves in Fluids*, Cambridge Univ. Press, New York.

Lupton, J., et al. (2006), Submarine venting of liquid carbon dioxide on a Mariana Arc volcano, *Geochem. Geophys. Geosyst.*, *7*, Q08007, doi:10.1029/2005GC001152.

Lupton, J. E., M. Lilley, D. A. Butterfield, L. Evans, R. W. Embley, G. Massoth, B. Christenson, K. Nakamura, and M. Schmidt (2008), Venting of a separate CO_2-rich gas phase from submarine arc volcanoes: Examples from the Mariana and Tonga-Kermadec arcs, *J. Geophys. Res.*, *113*, B08S12, doi:10.1029/2007JB005467.

Marty, B., and I. N. Tolstikhin (1998), CO_2 fluxes from mid-ocean ridges, arcs, and plumes, *Chem. Geol.*, *145*, 233–248, doi:10.1016/S0009-2541(97)00145-9.

McGonigle, A. J. S., A. Aiuppa, M. Ripepe, E. P. Kantzas, and G. Tamburello (2009), Spectroscopic capture of 1 Hz volcanic SO_2 fluxes and integration with volcano geophysical data, *Geophys. Res. Lett.*, *36*, L21309, doi:10.1029/2009GL040494.

Mori, T., P. A. Hernández, J. M. L. Salazar, N. M. Pérez, and K. Notsu (2001), An in situ method for measuring CO_2 flux from volcanic-hydrothermal fumaroles, *Chem. Geol.*, *177*, 85–99, doi:10.1016/S0009-2541(00)00384-3.

Mörner, N.-A., and G. Etiope (2002), Carbon degassing from the lithosphere, *Global Planet. Change*, *33*, 185–203, doi:10.1016/S0921-8181(02)00070-X.

Newhall, C. G., and S. Self (1982), The volcanic explosivity index (VEI): An estimate of explosive magnitude for historical volcanism, *J. Geophys. Res.*, *87*, 1231–1238, doi:10.1029/JC087iC02p01231.

Oshima, H., and T. Maekawa (2001), Excitation process of infrasonic waves associated with Merapi-type pyroclastic flow as revealed by a new recording system, *Geophys. Res. Lett.*, *28*, 1099–1102, doi:10.1029/1999GL010954.

Pecoraino, G., L. Brusca, W. D'Alessandro, S. Giammanco, S. Inguaggiato, and M. Longo (2005), Total CO_2 output from Ischia Island volcano (Italy), *Geochem. J.*, *39*, 451–458, doi:10.2343/geochemj.39.451.

Pérez, N. M., S. Nakai, K. Notsu, and B. Talai (1998), Anomalous diffuse degassing of helium-3 and CO_2 related to the active Ring-Fault structure at Rabaul Caldera, Papua New Guinea, *Eos Trans. AGU*, *79*(45), Fall Meet. Suppl., F957.

Resing, J. A., et al. (2007), Venting of acid-sulfate fluids in a high-sulfidation setting at NW Rota-1 submarine volcano on the Mariana Arc, *Econ. Geol.*, *102*(6), 1047–1061, doi:10.2113/gsecongeo.102.6.1047.

Resing, J. A., et al. (2011), Active submarine eruption of boninite in the northeastern Lau Basin, *Nat. Geosci.*, *4*, 799–806, doi:10.1038/ngeo1275.

Ripepe, M., E. Marchetti, and G. Ulivieri (2007), Infrasonic monitoring at Stromboli volcano during the 2003 effusive eruption: Insights on the explosive and degassing process of an open conduit system, *J. Geophys. Res.*, *112*, B09207, doi:10.1029/2006JB004613.

Rowe, C. A., et al. (2000), Seismic and acoustic observations at Mount Erebus Volcano, Ross Island, Antarctica, 1994–1998, *J. Volcanol. Geotherm. Res.*, *101*, 105–128, doi:10.1016/S0377-0273(00)00170-0.

Rubin, K. H., S. A. Soule, W. W. Chadwick Jr., D. J. Fornari, D. A. Clague, R. W. Embley, E. T. Baker, M. R. Perfit, D. W. Caress, and R. P. Dziak (2012), Volcanic eruptions in the deep sea, *Oceanography*, *25*(1), 142–157, doi:10.5670/oceanog.2012.12.

Salazar, M. L., P. A. Hernández, J. Alvarez, F. Segura, G. Melian, N. M. Perez, and K. Notzu (2000), Diffuse emission of CO_2 from Cerro Negro volcano, Nicaragua, Central America, paper presented at IAVCEI General Assembly 2000, Bali, Indonesia, 18–22 July.

Sano, Y., and S. N. Williams (1996), Fluxes of mantle and subducted carbon along convergent plate boundaries, *Geophys. Res. Lett.*, *23*, 2749–2752, doi:10.1029/96GL02260.

Shaw, A. M., et al. (2006), Volatile contents of NW Rota melt inclusions: Insight to explosive submarine arc volcanism, *Eos Trans. AGU*, *87*(52), Fall Meet. Suppl., Abstract V52B-05.

Shaw, A. M., et al. (2010), Deep pooling of low degree melts and volatile fluxes at the 85°E segment of the Gakkel Ridge: Evidence from olivine-hosted melt inclusions and glasses, *Earth Planet. Sci. Lett.*, *289*, 311–322, doi:10.1016/j.epsl.2009.11.018.

Siebert, L., and T. Simkin (2002), Volcanoes of the world: An illustrated catalog of Holocene volcanoes and their eruptions, *Global Volcanism Program Digital Inf. Ser., GVP-3*, Smithsonian Inst., Washington, D. C. [Available at http://www.volcano.si.edu/world/.]

Sparks, R. S. J. (1997), *Volcanic Plumes*, Wiley, New York.

Symonds, R. B., M. H. Reed, and W. I. Rose (1992), Origin, speciation, and fluxes of trace-element gases at Augustine volcano, Alaska: Insights into magma degassing and fumarolic processes, *Geochim. Cosmochim. Acta*, *56*, 633–657, doi:10.1016/0016-7037(92)90087-Y.

Symonds, R. B., W. I. Rose, G. Bluth, and T. M. Gerlach (1994), Volcanic-gas studies: Methods, results, and applications, in *Volatiles in Magmas: Mineralogical Society of America*, *Rev. Mineral.*, vol. 30, edited by M. R. Carroll and J. R. Holloway, pp. 1–66, Mineral. Soc. of Am., Chantilly, Va.

Talandier, J., and E. A. Okal (1987), Seismic detection of underwater volcanism: The example of French Polynesia, *Pure Appl. Geophys.*, *125*, 919–950, doi:10.1007/BF00879361.

Tunnicliffe, V., et al. (2009), Survival of mussels in extremely acidic waters on a submarine volcano, *Nat. Geosci.*, *2*, 344–348, doi:10.1038/ngeo500.

Urick, R. J. (1975), *Principles of Underwater Sound*, McGraw-Hill, New York.

Varley, N. R., and M. A. Armienta (2001), The absence of diffuse degassing at Popocatepetl volcano, Mexico, *Chem. Geol.*, *177*, 157–173, doi:10.1016/S0009-2541(00)00389-2.

Vergniolle, S., and G. Brandeis (1996), Strombolian explosions: 1. A large bubble breaking at the surface of a lava column as a source of sound, *J. Geophys. Res.*, *101*(B9), 20,433–20,448, doi:10.1029/96JB01178.

Vergniolle, S., G. Brandeis, and J.-C. Mareschal (1996), Strombolian explosions: 2. Eruption dynamics determined from acoustic measurements, *J. Geophys. Res.*, *101*(B9), 20,449–20,466, doi:10.1029/96JB01925.

Walker, S. L., et al. (2008), Eruption-fed particle plumes and volcaniclastic deposits at a submarine volcano: NW Rota-1 Mariana Arc, *J. Geophys. Res.*, *113*, B08S11, doi:10.1029/2007JB005441.

Wardell, L. J., P. R. Kyle, N. Dunbar, and B. Christenson (2001), White Island volcano, New Zealand: carbon dioxide and sulfur dioxide emission rates and melt inclusion studies, *Chem. Geol.*, *177*, 187–200, doi:10.1016/S0009-2541(00)00391-0.

Watts, A. B., C. Peirce, I. Grevemeyer, M. Pauletto, W. R. Stratford, D. Bassett, J. A. Hunter, L. M. Kalnins, and C. E. J. de Ronde (2012), Rapid rates of growth and collapse of Monowai submarine volcano in th Kermadec Arc, *Nat. Geosci.*, *5*(7), 510–515, doi:10.1038/ngeo1473.

Williams, S. N., et al. (1992), Global carbon dioxide emission to the atmosphere by volcanoes, *Geochim. Cosmochim. Acta*, *56*, 1765–1770, doi:10.1016/0016-7037(92)90243-C.

Wright, I. C., W. W. Chadwick Jr., C. E. J. De Ronde, D. Reymond, O. Hyvernaud, H.-H. Gennerich, P. Stoffers, K. Mackay, M. Dunkin, and S. C. Bannister (2008), Collapse and reconstruction of Monowai submarine volcano, Kermadec arc, 1998–2004, *J. Geophys. Res.*, *113*, B08S03, doi:10.1029/2007JB005138.

Zapata G., J. A., et al. (1997), SO_2 fluxes from Galeras Volcano, Colombia, 1989–1995: Progressive degassing and conduit obstruction of a Decade Volcano, *J. Volcanol. Geotherm. Res.*, *77*, 195–208, doi:10.1016/S0377-0273(96)00094-7.